Acta Crystallographica Section C
Crystal Structure Communications
ISSN 0108-2701

Hirshfeld surface analysis of two bendroflumethiazide solvates

Francesca P. A. Fabbiani,[a]* Charlotte K. Leech,[a] Kenneth Shankland,[a] Andrea Johnston,[b] Philippe Fernandes,[b] Alastair J. Florence[b] and Norman Shankland[b]

[a]ISIS Facility, Rutherford Appleton Laboratory, Chilton, Didcot, Oxon OX11 0QX, England, and [b]Strathclyde Institute for Biomedical Science, 27 Taylor Street, University of Strathclyde, Glasgow G4 0NR, Scotland
Correspondence e-mail: f.p.a.fabbiani@rl.ac.uk

Received 3 August 2007
Accepted 13 September 2007
Online 24 October 2007

Bendroflumethiazide, or 3-benzyl-6-(trifluoromethyl)-3,4-dihydro-2*H*-1,2,4-benzothiadiazine-7-sulfonamide 1,1-dioxide, is reported to crystallize as 1:1 solvates with acetone, $C_{15}H_{14}F_3N_3O_4S_2\cdot C_3H_6O$, and *N*,*N*-dimethylformamide, $C_{15}H_{14}F_3N_3O_4S_2\cdot C_3H_7NO$. A detailed investigation of the crystal packing and intermolecular interactions is presented by means of Hirshfeld surface analysis. This analysis confirms the atomic positions of methyl H atoms of the solvent molecules that were inferred from the X-ray data and provides a useful tool for structure validation.

Comment

Bendroflumethiazide (BFMZ) is a thiazide diuretic drug used in the treatment of hypertension. The work presented here forms part of a wider investigation that couples parallel crystallization searches (Florence *et al.*, 2006) with crystal structure prediction methodology to investigate the basic science underlying the solid-state diversity in thiazide diuretics, including chlorothiazide (Fernandes *et al.*, 2006, 2007) and hydrochlorothiazide (Johnston *et al.*, 2007).

The solvates, (I) and (II) (Figs. 1 and 2), were obtained by crystallization from acetone and *N*,*N*-dimethylformamide (DMF) solutions, respectively. Bond lengths and angles in the BFMZ group are not significantly different in the two crystal structures, but the molecular conformations are, reflecting the conformational freedom associated with the heterocyclic ring and benzyl group, as demonstrated in a structure overlay (Fig. 3) and in a comparison of the selected, widest varying, torsion angles (Table 1).

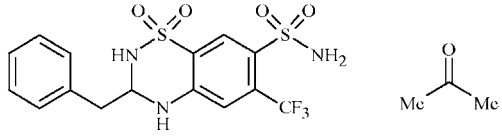

(I)

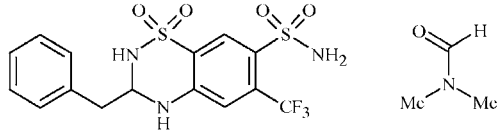

(II)

The hydrogen bonding in both structures is best described as three-dimensional and, unsurprisingly, the hydrogen-bonding patterns are quite distinct, with different hydrogen-bonding capabilities satisfied in the two structures (Table 2). Acceptors outnumber donors in both structures and it is therefore not surprising that atoms O1 (in both structures) and O4 (in the DMF solvate only) are unused. When longer and weaker hydrogen bonds are taken into consideration, both structures acquire one extra contact, giving rise to bifurcated hydrogen bonds [see Table 2 and Steiner (2000)]. A number of weaker C—H$\cdots\pi$ and C—H$\cdots$O interactions are also present in the two structures.

When comparing the same molecule in different crystal environments, Hirshfeld surfaces and fingerprint plots (McKinnon *et al.*, 1998, 2004; Spackman & McKinnon, 2002) have been shown to be a powerful tool for elucidating and comparing intermolecular interactions, complementing other tools currently available for the visualization of crystal struc-

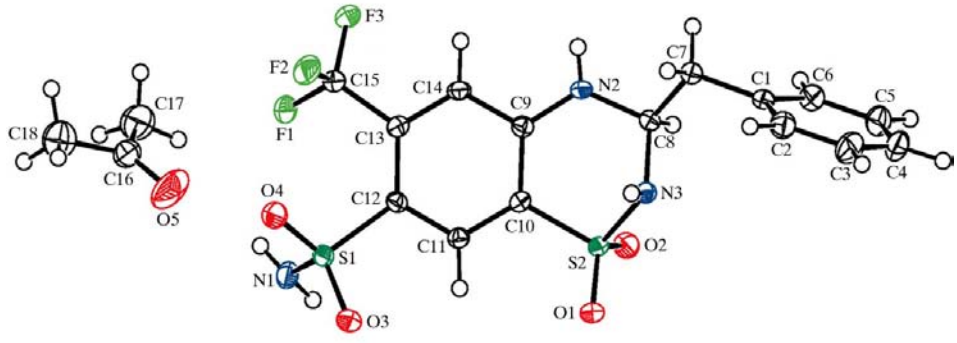

Figure 1
The BFMZ acetone solvate, (I), with displacement ellipsoids drawn at the 50% probability level. H atoms are shown as spheres of arbitrary radius.

 DOI: 10.1107/S0108270107044812

tures and for their systematic description and analysis, *e.g.* graph-set analysis (Etter *et al.*, 1990) and topological analysis (Blatov, 2006).

The number of Hirshfeld surfaces that are unique in a given crystal structure depends on the number of independent molecules in the asymmetric unit, implying that for the title compounds there are two resulting surfaces for each structure, *viz.* one for the solute and one for the solvent. Surfaces for BFMZ are shown in Figs. 4 and 5 (for the DMF solvate, a fully ordered BFMZ model was used); fingerprint plots for BFMZ and the solvents are shown in Fig. 6; d_e and d_i are defined as the distance from the surface to the nearest atom external and internal to the surface, respectively. A range of 0.8 (red in the electronic version of the paper) and 2.6 Å (blue) for mapping d_e on the surfaces was employed here. The surfaces are shown as transparent to allow visualization of the BFMZ group, in a similar orientation for both structures, around which they were calculated. It is clear that the information present in Table 2 is summarized effectively in these plots, with the large circular depressions (deep red in the electronic version of the paper) visible on the back and front views of the surfaces indicative of hydrogen-bonding contacts. The weak intra-molecular hydrogen bonds listed in Table 2 are, of course, not visible on the Hirshfeld surfaces, whereas weak hydrogen bonds where BFMZ is the acceptor are. The feature labelled 1 on the DMF fingerprint is indicative of a long C—H···O interaction [H···A = 2.65 Å, D···A = 3.590 (4) Å and D—H··· A = 170°], where DMF is the donor. The small extent of area and light colour of this feature on the surface in Fig. 5 indicates that this contact is weaker and longer than other hydrogen bonds. The interaction is not clearly visible in the

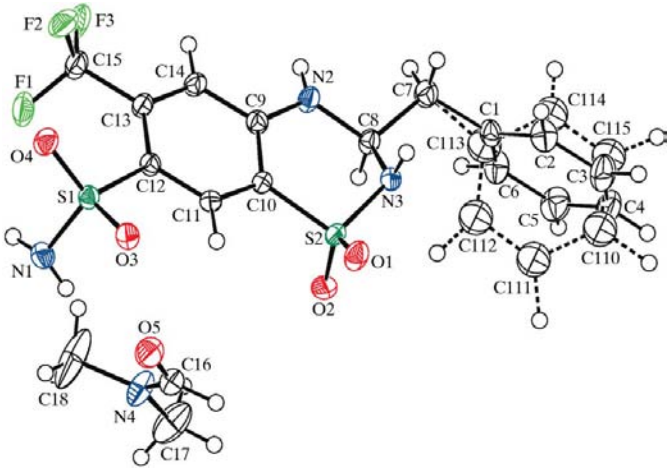

Figure 2
The BFMZ DMF solvate, (II), with displacement ellipsoids drawn at the 50% probability level. H atoms are shown as spheres of arbitrary radius. The minor disorder component is shown as dashed lines.

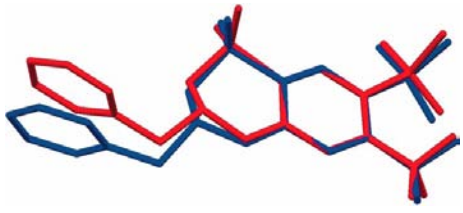

Figure 3
A structural overlay of the BFMZ groups in the DMF (light grey, or red in the electronic version of the paper) and acetone (dark grey, or blue in the electronic version) solvates, illustrating the different conformations adopted in the two crystal structures. Atoms overlaid: C9–C14, S1, C15; r.m.s. of overlay fit: 0.0515 Å.

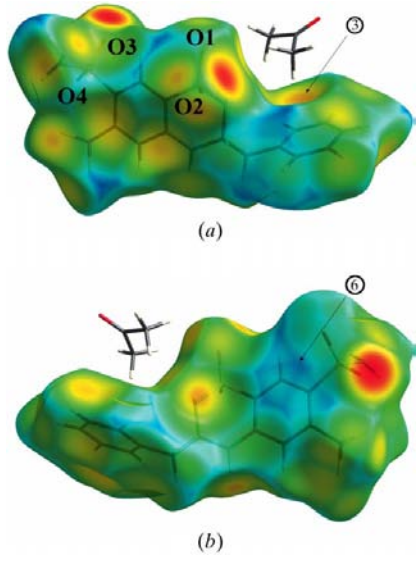

Figure 4
(*a*) Front and (*b*) back views of the Hirshfeld surface for BFMZ in the acetone solvate structure (Hirshfeld surface mapped with d_e). The labels are referred to in the *Comment*.

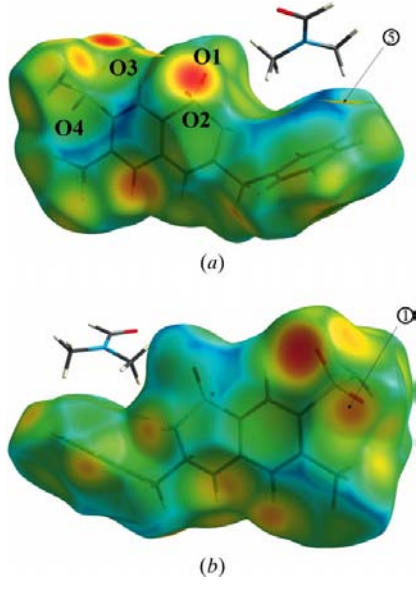

Figure 5
(*a*) Front and (*b*) back views of the Hirshfeld surface for BFMZ in the DMF solvate structure (Hirshfeld surface mapped with d_e). The labels are referred to in the *Comment*.

fingerprint of BFMZ as it overlaps with other interactions. The contact is clearly identifiable when the fingerprint is 'decomposed' into an H···O-interactions-only fingerprint (McKinnon & Spackman, 2007).

These fingerprint plots are quite asymmetric; this is because interactions occur between two chemically and crystallographically distinct molecules. Complementary regions are visible in the fingerprint plots where one molecule acts as a donor ($d_e > d_i$) and the other as an acceptor ($d_e < d_i$). Some complementary features are illustrated in Fig. 6, *e.g.* hydrogen bonding (labelled 2 – note that the spike in BFMZ is visibly thicker as more than one hydrogen bond is donated by BFMZ) and C—H···π interactions (labelled 3) between BFMZ and acetone, which are not present between BFMZ and DMF; C—H···π interactions within the BFMZ molecules are labelled 4.

The different conformations adopted by the BFMZ group can be partly understood in terms of favourable interactions formed with the two different solvents. The C—H···π interaction between BFMZ and acetone is visible in Fig. 4(*a*) as a deep large depression above the benzyl ring in the acetone solvate and is marked 3. The geometry of this interaction involves a H···*Cg* (*Cg* is the ring centroid) distance of 2.94 Å and a C—H···*Cg* bond angle of 166°. This interaction is not found between DMF and BFMZ in the DMF solvate, where a methyl H atom forms a close contact with a benzyl H atom instead, marked 5 in Fig. 5(*a*). This contributes to the observed 'tighter' conformation adopted by BFMZ in the DMF solvate.

The pattern of the flat region marked 6 (blue–green online) in Fig. 4(*b*) is characteristic of an offset π–π ring stacking. This is also labelled in Fig. 6(*a*); the $d_e = d_i \simeq 2.2$ Å distance is longer than the van der Waals separation typical of C atoms (*i.e.* near $d_e = d_i \simeq 1.8$ Å) owing to the presence of the trifluoromethyl group, which for steric reasons prevents the C atoms from coming into closer proximity.

During the final stages of crystal structure refinement of the DMF solvate, our attention was drawn to the quasi-staggered 50° torsion (see Fig. 7) of the methyl groups belonging to DMF. This contrasts with the fully eclipsed conformation found in the low-temperature structure of DMF (Borrmann *et al.*, 2000) and DFT (density functional theory) calculations on free DMF (Stålhandske *et al.*, 1997), which have shown that the fully staggered conformation is a transition state 9.6 kJ mol^{-1} less stable than the eclipsed state. Furthermore, the majority of DMF molecules in the Cambridge Structural Database (CSD; Version 5.28; Allen, 2002) (subset: organic only, not disordered, not polymeric, not ionic, *R* factor < 5%) lie in an eclipsed or nearly eclipsed conformation (*i.e.* 95 out of 117 entries with $\tau < 18°$, 22 out of 117 entries with $18 < \tau < 60°$).

Nevertheless, confidence in this observed conformation is high, the H-atom locations coming directly from Fourier maps. Placing the H atoms in calculated positions to give an eclipsed conformation generated very short H···H contacts, as shown in Fig. 8 (labelled 8). With DMF in the observed staggered conformation, the shortest H···H contacts are found at $d_e + d_i = 2.24$ Å, whilst for the eclipsed conformation, $d_e + d_i$ has the rather improbable value of 1.90 Å [*Crystal Explorer* (Wolff *et al.*, 2005) normalizes distances to H atoms to neutron values].[1] Furthermore, Fig. 8 also shows a more extended area of points at high values of d_e and d_i where points are scarce, indicating more extended void regions. This evidence overall suggests a more efficient packing adopted when DMF is in the staggered conformation. With the ability to interrogate fingerprint plots and Hirshfeld surfaces interactively, the unusually short contact is readily discernible as a C—H_{DMF}···H1—N_{BFMZ} contact.

The relatively contact-free space for the same H atom in the staggered DMF molecule could be interpreted either as a loss in number of contact points or as a relief from a close contact that arises at unfavourably short distances. A loss in number of contacts is offset by the gains to be realized with the formation of another favourable contact at 2.652 Å, namely a C18—H181···O4 interaction (labelled 1 in Fig. 5*b*). This favourable multi-point contact from CH in DMF towards the formation of strong and weak hydrogen bonds between the solvent and solute molecules has been cited as a contributing factor to why DMF tends to appear frequently as a solvate (Nangia & Desiraju, 1999).

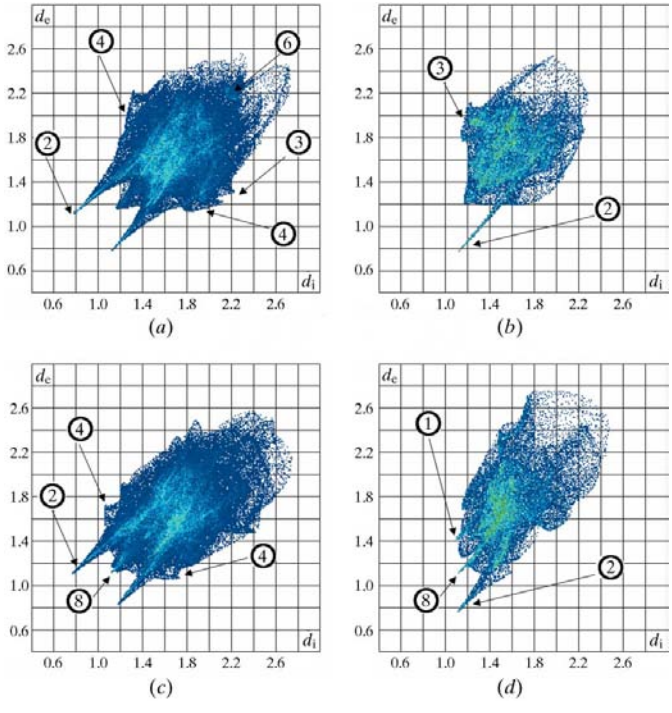

Figure 6
Fingerprint plots for BFMZ and solvent molecules in the acetone (*a*, *b*) and DMF (*c*, *d*) solvates. The labels are referred to in the *Comment*.

[1] Unusually short contacts are rare but not unknown. For example, a very short but real contact of $d_e = d_i = 1.02$ Å is observed in the crystal structure of pyrene II (Dunitz & Gavezzotti, 1999) and one at $d_e + d_i = 2.05$ Å has been recently identified in the Hirshfeld surface analysis of the OP polymorph of ROY (CSD refcode QAXMEH03; McKinnon & Spackman, 2007). To the best of our knowledge, the shortest intermolecular H···H contact in an organic crystal structure is that of the unstable polymorph of 1,2,3,5-tetra-*O*-acetyl-β-D-ribofuranose, with an H···H distance of 1.949 (7) Å (Bombicz *et al.*, 2003).

In a rapid structure validation exercise, we calculated fingerprint plots for the DMF molecules located in the CSD search and have found no striking anomalies in the fingerprint plots that might be due to incorrect conformation of the two methyl groups. Only one H···H contact below 2.0 Å (1.91 Å) involving methyl H atoms in DMF was found (CSD refcode PEWZOG; Bertha *et al.*, 1993), and for this structure, the staggered conformation gave an even closer contact of 0.78 Å. These results and the number of entries with torsion angles not equal to 0° indicate correct treatment of methyl H atoms during structural refinement of good-quality data, *e.g.* by determining the best torsion angle of an idealized CH_3 group, whilst retaining tetrahedral geometry.

Finally, this example underlines the utility of Hirshfeld surfaces and, in particular, fingerprint-plot analysis for the 'visual screening' and rapid detection of unusual crystal structure features (Fabbiani *et al.*, 2007) through a 'whole structure' view of intermolecular interactions (McKinnon *et al.*, 2004).

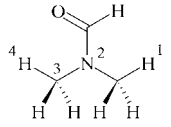

Figure 7
A molecular scheme of DMF; fully eclipsed methyl H atoms are defined at τ (1–2–3–4) = 0° and fully staggered at τ = 60°.

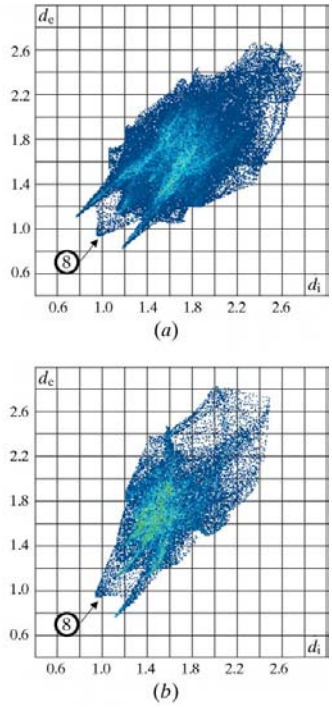

Figure 8
Fingerprint plots for (*a*) BFMZ and (*b*) the solvent molecule in the DMF solvate, with DMF methyl H atoms calculated in an eclipsed conformation. The labels are referred to in the *Comment*.

Experimental

BFMZ was obtained from Medex and used as received. Single crystals of the title compounds were obtained by slow evaporation at room temperature from saturated solutions in the respective solvents.

Compound (I)

Crystal data

$C_{15}H_{14}F_3N_3O_4S_2\cdot C_3H_6O$
M_r = 479.50
Triclinic, $P\overline{1}$
a = 8.192 (2) Å
b = 9.525 (2) Å
c = 14.101 (2) Å
α = 99.538 (17)°
β = 100.171 (17)°
γ = 100.42 (2)°
V = 1042.8 (4) Å^3
Z = 2
Mo $K\alpha$ radiation
μ = 0.32 mm^{-1}
T = 150 K
0.25 × 0.16 × 0.07 mm

Data collection

Oxford Diffraction Gemini diffractometer
Absorption correction: multi-scan (*CrysAlis RED*; Oxford Diffraction, 2006)
T_{min} = 0.97, T_{max} = 0.98
12169 measured reflections
4702 independent reflections
3973 reflections with $I > 2\sigma(I)$
R_{int} = 0.019

Refinement

$R[F^2 > 2\sigma(F^2)]$ = 0.033
$wR(F^2)$ = 0.079
S = 1.01
4702 reflections
292 parameters
H atoms treated by a mixture of independent and constrained refinement
$\Delta\rho_{max}$ = 0.36 e Å^{-3}
$\Delta\rho_{min}$ = −0.45 e Å^{-3}

Table 1
Selected torsion angles (°) for the solvates of BFMZ.

The same numbering scheme was adopted throughout the analysis. θ1(C2—C1—C7—C8), θ2(C11—C10—S2—N3) and θ3(C9—N2—C8—N3).

	θ_1	θ_2	θ_3
Acetone solvate, (I)	111.15 (18)	141.51 (13)	22.5 (2)
DMF solvate, (II)	99.0 (3)	157.37 (15)	39.0 (2)

Note: all standard uncertainties calculated with *PLATON* (Spek, 2003).

Compound (II)

Crystal data

$C_{15}H_{14}F_3N_3O_4S_2\cdot C_3H_7NO$
M_r = 494.51
Monoclinic, $P2_1/n$
a = 8.2527 (3) Å
b = 17.8431 (7) Å
c = 14.9012 (5) Å
β = 103.752 (4)°
V = 2131.35 (14) Å^3
Z = 4
Mo $K\alpha$ radiation
μ = 0.32 mm^{-1}
T = 150 K
0.19 × 0.09 × 0.07 mm

Data collection

Oxford Diffraction Gemini diffractometer
Absorption correction: multi-scan (*CrysAlis RED*; Oxford Diffraction, 2006)
T_{min} = 0.88, T_{max} = 0.98
28698 measured reflections
4615 independent reflections
3954 reflections with $I > 2\sigma(I)$
R_{int} = 0.034

Refinement

$R[F^2 > 2\sigma(F^2)]$ = 0.040
$wR(F^2)$ = 0.091
S = 1.01
4615 reflections
309 parameters
2 restraints
H atoms treated by a mixture of independent and constrained refinement
$\Delta\rho_{max}$ = 0.42 e Å^{-3}
$\Delta\rho_{min}$ = −0.46 e Å^{-3}

Table 2
Hydrogen-bond parameters (Å, °) for BFMZ DMF and acetone solvates.

D—H···A	D—H	H···A	D···A	D—H···A
DMF solvate				
N1—H100···O5$_{DMF}$	0.81 (2)	2.08 (2)	2.856 (2)	162 (2)
N1—H101···O2^{i}	0.89 (2)	2.23 (2)	3.050 (2)	152 (2)
N2—H102···O3^{ii}	0.81 (1)	2.31 (2)	3.040 (2)	151 (2)
N2—H102···O5$^{ii}_{DMF}$	0.81 (1)	2.72 (2)	3.291 (2)	129 (2)
N3—H103···O3^{iii}	0.85 (3)	2.18 (2)	3.008 (2)	168 (2)
Acetone solvate				
N1—H100···O2^{iv}	0.86 (2)	2.26 (2)	3.045 (2)	151.4 (18)
N1—H101···O5$_{acetone}$	0.82 (2)	2.10 (2)	2.901 (3)	166 (2)
N2—H102···O3^{v}	0.81 (2)	2.20 (2)	2.995 (2)	166 (2)
N2—H102···O2^{vi}	0.81 (2)	2.67 (2)	3.048 (2)	110.5 (16)
N3—H103···O4^{vii}	0.842 (19)	2.078 (19)	2.887 (2)	160.9 (18)

Notes: all standard uncertainties calculated with *PLATON* (Spek, 2003). Criteria for defining N—H···A interactions, as calculated by *PLATON*: $D\cdots A < R(D) + R(A)$, $H\cdots A < R(H) + R(A)$, D—H···$A > 100.0°$; $R(X)$ is the radius of atom X. Symmetry codes: (i) $x+\frac{1}{2}, -y+\frac{1}{2}, z+\frac{1}{2}$; (ii) $x-1, y, z$; (iii) $-x+1, -y+1, -z$; (iv) $-x+1, -y+2, -z+1$; (v) $x+1, y, z$; (vi) $-x+2, -y+2, -z+1$; (vii) $-x+1, -y+1, -z+1$.

All non-H atoms were modelled with anisotropic displacement parameters, with the exception of the minor component of the disordered site in the DMF solvate, for which one common isotropic displacement parameter was refined. H atoms were located in a difference Fourier map. The program *CRYSTALS* (Betteridge *et al.*, 2003) allowed initial refinement of H-atom positions using the X-ray data and soft restraints on bond lengths and angles to regularize their geometry. U_{iso}(H) values were assigned in the range 1.2–1.5 times U_{eq} of the parent atom. H atoms were subsequently allowed to ride on their parent atoms, with the exception of those attached to N atoms, whose positions were freely refined.

In the structure of the DMF solvate, unusually high peaks were observed in the final difference Fourier maps in the proximity of the terminal benzene ring, clearly indicating disorder of this group over a further site. Given the distorted geometry of the secondary orientation, the ring was refined as a rigid group subsequent to geometry regularization. Distance and bond-angle restraints were used to ensure a reasonable orientation of this group with respect to the main ordered group, and to mimic rotation of the group about the C1—C7 axis. The occupancies of the two components refined to 0.934 (3) and 0.066 (3). Inclusion of the disorder model contributed to a significant improvement of the *R* factor as well as of the difference Fourier maps. A common isotropic displacement parameter was refined for the C atoms belonging to the secondary component and the disordered H atoms were placed in calculated positions.

For both compounds, data collection: *CrysAlis CCD* (Oxford Diffraction, 2006); cell refinement: *CrysAlis CCD*; data reduction: *CrysAlis CCD*. Program(s) used to solve structure: *SHELXS97* (Sheldrick, 1990) for (I); *SIR92* (Altomare *et al.*, 1993) for (II). For both compounds, program(s) used to refine structure: *CRYSTALS* (Betteridge *et al.*, 2003); molecular graphics: *ORTEP-3* (Farrugia, 1997), *Crystal Explorer* (Wolff *et al.*, 2005) and *Mercury* (Macrae *et al.*, 2006); software used to prepare material for publication: *PLATON* (Spek, 2003) and *publCIF* (Westrip, 2007).

The authors thank the Basic Technology Programme of the UK Research Councils for funding this work under the project Control and Prediction of the Organic Solid State (http://www.cposs.org.uk). We also thank Dr J. J. McKinnon (University of Western Australia) for his help with *Crystal Explorer*.

Supplementary data for this paper are available from the IUCr electronic archives (Reference: BM3035). Services for accessing these data are described at the back of the journal.

References

Allen, F. H. (2002). *Acta Cryst.* B**58**, 380–388.
Altomare, A., Cascarano, G., Giacovazzo, C. & Guagliardi, A. (1993). *J. Appl. Cryst.* **26**, 343–350.
Bertha, F., Fetter, J., Kajtar-Peredy, M., Keseru, G. M., Lempert, K., Parkanyi, L. & Tamas, J. (1993). *Tetrahedron*, **49**, 7803–7822.
Betteridge, P. W., Carruthers, J. R., Cooper, R. I., Prout, K. & Watkin, D. J. (2003). *J. Appl. Cryst.* **36**, 1487.
Blatov, V. A. (2006). *Acta Cryst.* A**62**, 356–364.
Bombicz, P., Czugler, M., Tellgren, R. & Kálmán, A. (2003). *Angew. Chem. Int. Ed.* **42**, 1957–1960.
Borrmann, H., Persson, I., Sandström, M. & Stålhandske, C. M. V. (2000). *J. Chem. Soc. Perkin Trans. 2*, pp. 393–402.
Dunitz, J. D. & Gavezzotti, A. (1999). *Acc. Chem. Res.* **32**, 677–684.
Etter, M. C., MacDonald, J. C. & Bernstein, J. (1990). *Acta Cryst.* B**46**, 256–262.
Fabbiani, F. P. A., Byrne, L. T., McKinnon, J. J. & Spackman, M. A. (2007). *CrystEngComm*, **9**, 728–731.
Farrugia, L. J. (1997). *J. Appl. Cryst.* **30**, 565.
Fernandes, P., Florence, A. J., Shankland, K., Shankland, N. & Johnston, A. (2006). *Acta Cryst.* E**62**, o2216–o2218.
Fernandes, P., Shankland, K., Florence, A. J., Shankland, N. & Johnston, A. (2007). *J. Pharm. Sci.* **96**, 1192–1202.
Florence, A. J., Johnston, A., Fernandes, P., Shankland, N. & Shankland, K. (2006). *J. Appl. Cryst.* **39**, 922–924.
Johnston, A., Florence, A. J., Shankland, N., Kennedy, A. R., Shankland, K. & Price, S. L. (2007). *Cryst. Growth Des.* **7**, 705–712.
McKinnon, J. J. & Spackman, M. A. (2007). *Chem. Commun.* pp. 3814–3816.
McKinnon, J. J., Spackman, M. A. & Mitchell, A. S. (1998). *Chem. Eur. J.* **4**, 2136–2141.
McKinnon, J. J., Spackman, M. A. & Mitchell, A. S. (2004). *Acta Cryst.* B**60**, 627–668.
Macrae, C. F., Edgington, P. R., McCabe, P., Pidcock, E., Shields, G. P., Taylor, R., Towler, M. & van de Streek, J. (2006). *J. Appl. Cryst.* **39**, 453–457.
Nangia, A. & Desiraju, G. R. (1999). *Chem. Commun.* pp. 605–606.
Oxford Diffraction (2006). *CrysAlis CCD*. Version 1.171.31.5. Oxford Diffraction Ltd, Abingdon, Oxfordshire, England.
Sheldrick, G. M. (1990). *Acta Cryst.* A**46**, 467–473.
Spackman, M. A. & McKinnon, J. J. (2002). *CrystEngComm*, **4**, 378–392.
Spek, A. L. (2003). *J. Appl. Cryst.* **36**, 7–13.
Stålhandske, C. M. V., Mink, J., Sandström, M., Papai, I. & Johansson, P. (1997). *Vib. Spectrosc.* **14**, 207–227.
Steiner, T. (2000). *Angew. Chem. Int. Ed.* **41**, 48–76.
Westrip, S. P. (2007). *publCIF*. In preparation.
Wolff, S. K., Grimwood, D., McKinnon, J., Jayatilaka, D. & Spackman, M. (2005). *Crystal Explorer*. Version 1.5. University of Western Australia, Australia.